frontiers in Earth Science

ORIGINAL RESEARCH
published: 15 May 2019
doi: 10.3389/feart.2019.00097

Fire Responses to the 2010 and 2015/2016 Amazonian Droughts

Celso H. L. Silva Junior[1,2], Liana O. Anderson[1,3], Alindomar L. Silva[2], Catherine T. Almeida[1,2], Ricardo Dalagnol[1,2], Mikhaela A. J. S. Pletsch[2], Thales V. Penha[2], Rennan A. Paloschi[2] and Luiz E. O. C. Aragão[1,2,4]*

[1] Tropical Ecosystems and Environmental Sciences Laboratory, São José dos Campos, Brazil, [2] National Institute for Space Research, São José dos Campos, Brazil, [3] National Center for Monitoring and Early Warning of Natural Disasters, São José dos Campos, Brazil, [4] College of Life and Environmental Sciences, University of Exeter, Exeter, United Kingdom

Extreme droughts in Amazonia cause anomalous increase in fire occurrence, disrupting the stability of environmental, social, and economic systems. Thus, understanding how droughts affect fire patterns in this region is essential for anticipating and planning actions for remediation of possible impacts. Focused on the Brazilian Amazon biome, we investigated fire responses to the 2010 and 2015/2016 Amazonian droughts using remote sensing data. Our results revealed that the 2015/2016 drought surpassed the 2010 drought in intensity and extent. During the 2010 drought, we found a maximum area of 846,800 km^2 (24% of the Brazilian Amazon biome) with significant ($p \leq 0.05$) rainfall decrease in the first trimester, while during the 2015/2016 the maximum area reached 1,702,800 km^2 (47% of the Brazilian Amazon biome) in the last trimester of 2015. On the other hand, the 2010 drought had a maximum area of 840,400 km^2 (23% of the Brazilian Amazon biome) with significant ($p \leq 0.05$) land surface temperature increase in the first trimester, while during the 2015/2016 drought the maximum area was 2,188,800 km^2 (61% of the Brazilian Amazon biome) in the last trimester of 2015. Unlike the 2010 drought, during the 2015/2016 drought, significant positive anomalies of active fire and CO_2 emissions occurred mainly during the wet season, between October 2015 and March 2016. During the 2010 drought, positive active fire anomalies resulted from the simultaneous increase of burned forest, non-forest vegetation and productive lands. During the 2015/2016 drought, however, this increase was dominated by burned forests. The two analyzed droughts emitted together 0.47 Pg CO_2, with 0.23 Pg CO_2 in 2010, 0.15 Pg CO_2 in 2015 and 0.09 Pg CO_2 in 2016, which represented, respectively, 209%, 136%, 82% of annual Brazil's national target for reducing carbon emissions from deforestation by 2017 (approximately 0.11 Pg CO_2 year^{-1} from 2006 to 2017). Finally, we anticipate that the increase of fires during the droughts showed here may intensify and can become more frequent in Amazonia due to changes in climatic variability if no regulations on fire use are implemented.

Keywords: old-growth forest, temperature, rainfall, remote sensing, CHIRPS, MODIS, GFEDv4

OPEN ACCESS

Edited by:
Juan Carlos Jimenez, University of Valencia, Spain

Reviewed by:
José Manuel Moreno, Universidad de Castilla-La Mancha, Spain
Cristian Mattar, Universidad de Aysen, Chile

****Correspondence:***
Celso H. L. Silva Junior
celso.junior@inpe.br

Specialty section:
This article was submitted to Interdisciplinary Climate Studies, a section of the journal Frontiers in Earth Science

Received: *22 September 2018*
Accepted: *18 April 2019*
Published: *15 May 2019*

Citation:
Silva Junior CHL, Anderson LO, Silva AL, Almeida CT, Dalagnol R, Pletsch MAJS, Penha TV, Paloschi RA and Aragão LEOC (2019) Fire Responses to the 2010 and 2015/2016 Amazonian Droughts. Front. Earth Sci. 7:97. doi: 10.3389/feart.2019.00097

INTRODUCTION

Tropical forests host between 20 and 40% of the known animals and plant species of the globe (Maués and Oliveira, 2010). Among them, the Amazon rainforest stands out for its rich biodiversity and for playing a crucial role on climate regulation and global carbon cycle (Marengo and Betts, 2011). Nevertheless, extreme droughts, such as those caused by the El Niño Southern Oscillation (ENSO) and the Atlantic Multidecadal Oscillation (AMO), are able to cause priceless environmental, social and economic damages (Anderson et al., 2011; Smith et al., 2014; Marengo and Espinoza, 2016; Silva Junior et al., 2018a; Campanharo et al., 2019). Here, we consider as drought, the year in which rainfall is significantly below the expected average, resulting in significant abnormally low rainfall. During the last century, the Amazon region underwent eight major droughts, with a mean interval of 12 years. However, just in the first 16 years of this century, the region has already experienced four major droughts, with a mean interval of only 4 years (Marengo and Espinoza, 2016). The occurrence of these repeated droughts in such short time evidences the climate change effects, which were already predicted for the 21st century by global models (Li et al., 2006; Malhi et al., 2008).

The occurrence of frequent and severe droughts negatively affect the structure and function of Amazonian ecosystems, impacting the forest carbon balance through reduced forest productivity and increased tree mortality (Phillips et al., 2009; Brienen et al., 2015; Anderson et al., 2018) and increasing forest's vulnerability to fire (Aragão et al., 2007, 2018). According to Aragão et al. (2014), carbon emissions during drought years could double (from 0.24 to 0.46 Pg C year^{-1}) as a direct result of the increase in forest fires and tree mortality. Besides that, according to Aragão et al. (2018), carbon emissions from forest fires alone during drought years are more than half as great as those from old-growth forest deforestation.

In Amazonia, fire seasonality is the result of a synergic interaction between deforestation, vegetation water deficit, and ignition sources (Aragão et al., 2008; Cochrane and Laurance, 2008; Cano-Crespo et al., 2014; Fanin and van der Werf, 2015). In this region, fires can be classified into three categories, related to their origin (Aragão et al., 2008; Lima et al., 2012): (a) areas that have been deforested and then burned in the same year, (b) areas that have been deforested in previous years and then burned, such as management of agricultural and livestock areas, and (c) fires in natural vegetation cover, as in forest and savannas. However, due to the increased frequency of droughts in Amazonia (Marengo et al., 2011, 2018; Marengo and Betts, 2011; Jiménez-Muñoz et al., 2016; Marengo and Espinoza, 2016; Garcia et al., 2018), the incidence of fires has been exacerbated in the region (Aragão et al., 2007, 2018). Drought-affected areas are more prone to fire occurrence due to increased vegetation water deficit. Water deficits increase fuel availability by drying the pre-existent necromass and litter within the forest understory, as dead trunks, branches and leaves, and also potentially kill trees through natural processes that add up to the fuel stock (Anderson, 2012; Aragão et al., 2014). On the other hand, although droughts tend to increase fire probability in forests, the spatial pattern of drought-induced fires is consistent with the distribution of human settlements that act as ignition sources within Amazonia region (Aragão et al., 2007).

Since fire occurrence can be enhanced by droughts, its effects vary accordingly to the spatial and temporal distribution of these droughts. Considering recent drought events that occurred in Amazonia, it is clear that each one has distinct spatial and temporal patterns following the configuration of a variety of climate controlling factors (Aragão et al., 2007, 2018; Marengo et al., 2011; Coelho et al., 2012; Jiménez-Muñoz et al., 2016; Marengo and Espinoza, 2016; Panisset et al., 2018). In the year 2005, for instance, the drought was primarily reported as a direct consequence of the North Tropical Atlantic Ocean warming, affecting mainly the southwest region of the Amazon forest (Aragão et al., 2007). On the other hand, the 2010 drought was associated with both the North Tropical Atlantic Ocean warming and the ENSO, impacting not only the southwest region but also the south region (Marengo et al., 2011). Recently, at the end of 2015 and the first months of 2016, one of the greatest El Niño events of the last decades was registered; and it was associated with an increase in land surface temperatures, associated to an intense period of drought in central Amazonian forests (Jiménez-Muñoz et al., 2016). However, the spatial-temporal pattern of fire occurrences in 2016 year during 2015/2016 drought has not been investigated in the literature.

Therefore, in order to help mitigating the negative effects of fires upon Amazonian forests and better prepare the society, living in vulnerable areas, to cope with the impacts of drought and fire under a changing climate, it is necessary to understand the different causes and patterns associated with droughts and how these droughts impact the patterns of fire occurrence in Amazonia. Aragão et al. (2007) analyzed the spatial extent of the 2005 Amazonian drought and its associated fire response. The results showed that, during 2005, the annual cumulative number of thermal anomalies (an indicator of active fire) increased 33% in relation to the 1999–2005 mean in Amazonia.

To expand the analysis provided by Aragão et al. (2007), we investigated the different causes and patterns associated with the 2010 and 2015/2016 Amazonian droughts and their impacts on fire occurrence and carbon emissions in the Brazilian Amazon biome. In this study, we aim to answer the following questions: (1) What are the causes and the spatio-temporal patterns of intra-annual rainfall and temperature anomalies during the 2010 and 2015/2016 Amazonia droughts? (2) What is the spatio-temporal response of fire occurrence during the 2010 and 2015/2016 Amazonian droughts? (3) What is the extent of burned forest, non-forest vegetation and productive lands during the 2010 and 2015/2016 Amazonian droughts, and their fire-associated carbon dioxide (CO_2) emissions?

MATERIALS AND METHODS

Study Area

The study area encompasses the Brazilian Amazon biome (**Figure 1**) (Instituto Brasileiro de Geografia e Estatística [IBGE], 2004; Ministério do Meio Ambiente [MMA], 2018). This region

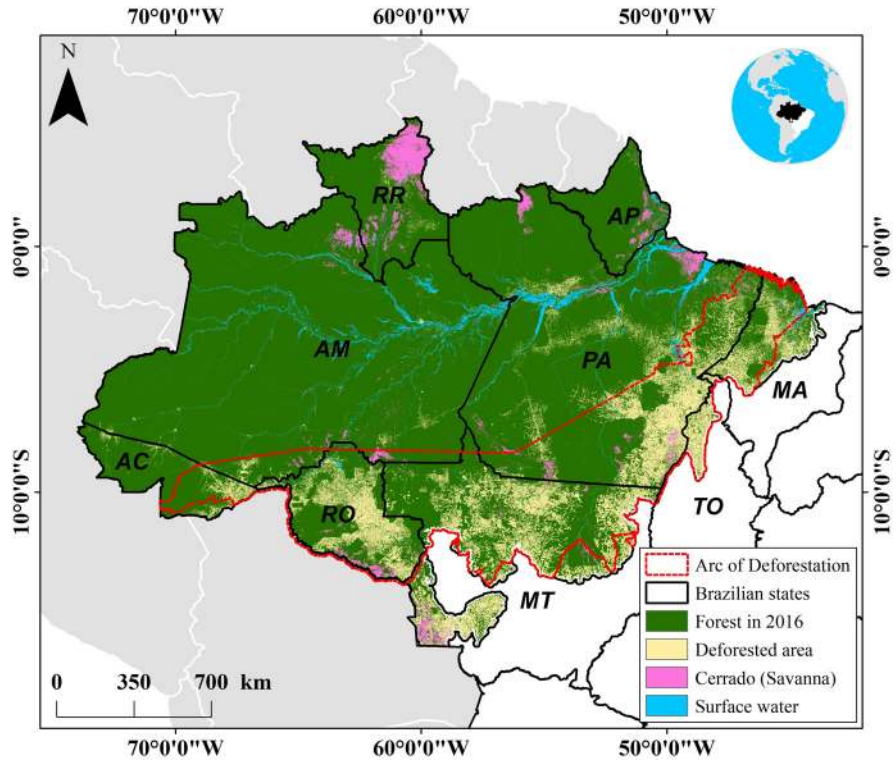

FIGURE 1 | Location map of the study area. On the main map, in green are the old-growth and secondary forests, in yellow non-forest areas and in blue the surfaces water. The Land-cover data for the year 2016 were obtained from the MapBiomas Project (http://mapbiomas.org). Brazilian States: AC, Acre; AM, Amazonas; AP, Amapá; MA, Maranhão; MT, Mato Grosso; PA, Pará; RO, Rondônia; RR, Roraima; TO, Tocantins.

covers an area of 4,196,943 km^2, which represent 49% of the Brazilian territory. Forest areas in the Brazilian Amazon biome declined from 3.856.867 km^2 in 1985 to 3.493.163 km^2 in 2017 (MapBiomas, 2018). The period analyzed in this research refers to the 2006–2016 period, a window of 11 years affected by two major droughts, in 2010 and 2015/2016 (Jiménez-Muñoz et al., 2016; Aragão et al., 2018). This time interval also corresponds to a period with the stabilization of deforestation rates in the Brazilian Amazon biome at low historical levels (Instituto Nacional de Pesquisas Espaciais [INPE], 2018). By focusing on the studied period, we aimed to reduce the influence of fires directly associated with the deforestation process.

The Brazilian Amazon biome plays a key role in worldwide climate regulation and in preserving fundamental ecosystem services (Nepstad et al., 2009; Aragão et al., 2014). Among the challenges faced by the region, those related to land transformation for different purposes stand out, such as deforestation and fires. Historically, cattle ranching and agriculture are the main drivers of Amazonia's land cover and land use changes (Fearnside, 2005). This is evident in the active land-use frontier in southern Amazonia (Morton et al., 2006), known as Arc of Deforestation, which is consolidated in terms of forest losses, intensity of fire activity and expansion of economic activities (Kalamandeen et al., 2018). This region is located in the Equatorial climate zone A, according to Köppen climate classification (Köppen, 1936). This climate zone is characterized by constant high temperatures, with the temperature of the coldest month being 18°C or higher (Kottek et al., 2006). As a whole, Amazonia comprehends three main tropical climatic zones: Equatorial Rainforest (Af) in the northwest, the Equatorial Monsoon (Am) observed in the center, and the Equatorial Savannah climate with dry winter (Aw), located at the eastern and southern flanks of the region (Alvares et al., 2013). Amazonia also embraces a small portion of the Equatorial Savannah with dry summer (As) in the extreme northern region of the Maranhão state (Alvares et al., 2013).

Datasets

Sea Surface Temperature Anomalies

We analyzed 11 years of monthly time-series (2006–2016) of Atlantic and Pacific sea surface temperature anomalies indices[1], acquired from the National Oceanic and Atmospheric Administration – NOAA. Positive sea surface temperature anomalies have been associated with the intensification of negative rainfall anomalies in the Amazon (Aragão et al., 2018). The first index evaluated was the Multivariate El Niño Index (MEI). The MEI index anomalies are composed of six variables collected over the Pacific Ocean, used to characterize the Southern Oscillation (ENSO) phenomenon (Wolter, 1987). Negative values of the MEI represent the

[1]http://www.esrl.noaa.gov/psd/data/climateindices/list

cold ENSO phase (La Niña), while positive values represent the warm phase (El Niño). Very intense El Niño has been associated with droughts in the Amazon region (Marengo et al., 2016). Secondly, we evaluated the Pacific Decadal Oscillation Index (PDO). The PDO depicts long-term patterns of El Niño-like status of the Pacific Ocean (Zhang et al., 1997). Positive PDO indicates the warm phase of the Pacific, and the opposite reflects the cold phase. Finally, we assessed the Atlantic Multidecadal Oscillation index (AMO), which describes average anomalies of sea surface temperatures (SST) in the North Atlantic basin, typically over 0–70N (Schlesinger and Ramankutty, 1994). The AMO index was acquired from the *Kaplan SST V2* from the *NOAA/OAR/ESRL PSD, Boulder, CO, United States,* covering the extent of 87.5°S – 87.5°N, 2.5°E – 357.5°E.

Rainfall

We used the monthly precipitation data from the Climate Hazards Group InfraRed Precipitation with Station data (CHIRPS; Funk et al., 2015). CHIRPS is a rainfall product and is made available at daily to seasonal time scales with a spatial resolution of 0.05°, starting from 1981 onward[2]. The CHIRPS rainfall dataset incorporates satellite information with *in situ* rainfall gauge station data to create gridded rainfall time series. This dataset has shown good performance in several regions of the world (Lopez-Carr et al., 2015; Duan et al., 2016; Katsanos et al., 2016; Verdin et al., 2016; Correa et al., 2017; Perdigón-Morales et al., 2018) and explains about 73% of observed rainfall in field gauge stations in the Brazilian Amazon with a root mean square error below 15 mm month^{-1} (Anderson et al., 2018).

Land Surface Temperature

The surface temperature data was derived from MODIS MOD11C3 (Collection 6) (Wan et al., 2015). This product is available for the entire globe in a spatial resolution of 0.05° and is calculated from the daily mean temperature of the MOD11C1 product[3]. Calibration of the product is often carried out using fieldwork data and studies based on radiance (Wan et al., 2015). The Collection 6 shows improvements regarding aerosol and cloud content (Wan et al., 2015).

Land Use and Land Cover

We used land use and land cover data from the Brazilian Annual Land Use and Land Cover Mapping Project (Collection 3[4]) (MapBiomas, 2018). This dataset is based on the classification of Landsat images (30m of spatial resolution) using a theoretical algorithm implemented in a cloud computing platform. Details about the processing and validation of the dataset can be found in the Algorithm Theoretical Basis Document[5]. The accuracy estimation for Collection 3 is still in preparation and as soon as it is completed it will be available at: http://mapbiomas.org/pages/accuracy-analysis. However, the last overall accuracy of the maps (Collection 2.3) provided by the MapBiomas for the Amazon biome was 82.70%.

Active Fire

We acquired the active fire data from MODIS sensor onboard AQUA satellite, which is available online at FIRMS – *Fire Information for Resource Management System*[6]. The data is derived from the active fire product from MODIS MCD14ML (Collection 6), where all active fires are adjusted to a spatial resolution of 1 km. Here, we used only the active fires with 80% or higher confidence level.

This product is created through a contextual algorithm that compares the medium and thermal infrared bands with reference images without fire. Following the comparison, false detections are rejected by the brightness temperature test in relation to its neighbor pixels (Giglio et al., 2003).

In Collection 6, the MODIS MCD14ML product quality has improved quite significantly and now commits less commission and omission errors in tropical ecosystems, and is able to identify smaller fires (Giglio et al., 2016). This product had global commission error of 1.20%, indicating improvements in the performance of the Collection 6 compared to Collection 5 (Giglio et al., 2016).

Burned Area

We acquired burned area data from the new global burned area product[7] developed by European Space Agency's (ESA) Climate Change Initiative (CCI) program, under the Fire Disturbance project (Fire_cci). The ESA burned area product has spatial resolution of 250 m with an estimated overall accuracy of 0.99, omission error of 0.70 and commission error of 0.51 (Chuvieco et al., 2018).

The burned area detection algorithm is based on monthly composites of daily images (MODIS MOD09GQ surface reflectance product), using temporal and spatial distances from active fires (MODIS MCD14ML active fire product). Two steps are considered in the algorithm. The first aims to reduce commission errors by selection of clearly burned pixels and uses active fires as seeds to its detection. The second one, which aims to reduce omission errors, is based on an application of contextual analysis around the seed pixels (Chuvieco et al., 2018).

Carbon Dioxide (CO_2) Emissions

We used the CO_2 emission data from the Global Fire Emissions Database (GEFEDv4[8]). This data is available at a spatial resolution of 0.25° (Van Der Werf et al., 2017). The GEFEDv4 dataset combines information from satellite data, regarding fire activity and vegetation productivity. This dataset is based upon large and small areas affected by fire (Randerson et al., 2012; Giglio et al., 2013; Van Der Werf et al., 2017). The emissions are estimated using the methods employed in the literature (Andreae and Merlet, 2001; Van Der Werf et al., 2010, 2017; Akagi et al., 2011).

[2]http://chg.geog.ucsb.edu/data/chirps/

[3]https://search.earthdata.nasa.gov

[4]http://mapbiomas.org/pages/database/mapbiomas_collection

[5]http://mapbiomas.org/pages/atbd

[6]https://earthdata.nasa.gov/earth-observation-data/near-real-time/firms/

[7]https://doi.org/cpk7

[8]http://www.globalfiredata.org

Methods

Data Processing

First, we resampled the rainfall and surface temperature data to a spatial resolution of 0.20° using the nearest neighbor average. Afterward, we quantified the monthly active fire occurrence using pixels in a grid cell coincident with the rainfall and surface temperature grid.

To perform the temporal monthly analysis, we calculated the average of all pixels within the boundaries of the Brazilian Amazon biome for surface temperature and rainfall data, followed by the quantification of all active fire occurrences and total CO_2 emissions using the same temporal scale. Then, to perform the spatial analysis, the data was grouped in four trimesters: January, February and March (JFM); April, May, and June (AMJ); July, August, and September (JAS), and October, November, and December (OND). For the surface temperature data, the values were aggregated considering the mean value. For both rainfall and active fire data, the sum within each trimester was considered.

Burned Area by Land Use and Land Cover

First, we use monthly burned area data to compile 11 annual burned area maps (2006–2016). Then, we resampled the annual burned areas data to a spatial resolution of 30 m to match the land use and land cover data. Finally, we simplified the original classes of the land use and land cover data, resulting in the following three new classes: Forest (Forest Formations), Non-Forest Vegetation (Grassland and Others Non-Forest Formation), and Productive Lands (Agriculture, Pasture and Agriculture/Pasture). The other classes of the land use and land cover data were not considered in our analyses. To quantify the burned areas by land use and land cover classes, we overlay the maps year by year.

Anomalies Calculation and Analysis

We calculated monthly and three-monthly period anomalies using Eq. (1) (Aragão et al., 2007). The anomalies were given by the normalized standard deviation (σ). For calculating the average and standard deviation, we excluded the years of 2010, 2015, and 2016.

$$X_{Anomaly} = \frac{\left(X_i - \bar{X}_{2006-2016}\right)}{\sigma_{2006-2016}} \quad (1)$$

In Eq. (1), X is the month or three-monthly period under analysis, $\bar{X}$ the monthly or quarterly average of the 2006–2016 temporal series, and σ is the standard deviation of the 2006–2016 temporal series. We considered as significant anomalies those higher or equal to 1.96 and lower or equal to −1.96 standard deviation, which corresponds to a confidence level of 95% (Anderson et al., 2010).

To assess the recurrence of rainfall, temperature, and fire anomalies in the two droughts evaluated, we considered only the areas with significant negative anomalies ($p \leq 0.05$) for rainfall and positive for temperature and fire. First, we assign the value 1 to these areas, resulting in binary maps, which were summed to obtain the recurrences for each trimester. Finally, we quantify the proportion of pixels with significant positive fire anomalies ($p \leq 0.05$) associated with significant decrease of rainfall, increase of temperature or both ($p \leq 0.05$).

RESULTS

Temporal Patterns of the Sea Surface Temperature Anomalies and Their Relationship With Rainfall, Temperature, and Fire Occurrence

During 2010, the MEI had positive anomalies in the beginning of the year, turning subsequently into negative values (**Figure 2A**). The AMO index had positive anomalies throughout the year (**Figure 2C**). The PDO was neutral and turned into negative values (**Figure 2B**). During this year, in addition to the decrease in rainfall (**Figure 2D**), we observed an increase in temperature (**Figure 2E**) and fire anomalies (**Figure 2F**). In 2015, differently, the three oceanic indices exhibited positive anomalies (**Figures 2A–C**), developing the longest period with abnormally low rainfall (**Figure 2D**) and high temperatures (**Figure 2E**), while fires also peaked (**Figure 2F**). Interestingly, both MEI (**Figure 2A**) and PDO (**Figure 2B**) indices decreased in 2016, presenting negative anomalies, with an increase in rainfall (**Figure 2D**), followed by a decrease in fire (**Figure 2F**) and temperatures anomalies (**Figure 2E**). Toward the end of 2016, rainfall increased (**Figure 2D**), followed by the decrease in land surface temperature (**Figure 2E**), and a cessation of positive fire anomalies (**Figure 2F**). It is remarkable that the highest significant positive fire anomalies ($p \leq 0.05$) were observed in December 2015 (4.46 σ), January (17.13 σ), and March (4.33 σ) 2016, when most of the Amazon Biome is usually under the wet season. However, significant negative rainfall anomalies ($p \leq 0.05$) persisted from September 2015 (−3.51 σ) to February 2016 (−3.97 σ).

Spatial Patterns of Rainfall, Temperature, and Fire Anomalies

Rainfall Anomalies

Regarding the impacted areas, we observed that the spatial distribution of 2010, 2015, and 2016 droughts was remarkably different (**Figure 3**). During the JFM period of 2010 and 2016, the significant negative rainfall anomalies were accumulated in the north portion, especially in Amazonas and Pará states, corresponding to 24% (846,800 km^2) and 19% (670,400 km^2) of the total study area, respectively. On the other hand, in 2015, we found significant negative rainfall anomalies in the southern and central region of Amazonia as well as in the northern portion of Pará and Rondônia states, affecting all together about 7% (248,000 km^2) of the total study area.

During the period of AMJ, which corresponds to the beginning of the dry season, we observed the development of large areas with significant negative rainfall anomalies in 2010 and 2016, mainly in the south region, corresponding to 13% (452,000 km^2) and 8% (272,400 km^2) of the study area, respectively. However, we also noted a small area of significant negative rainfall anomalies in the northern region in 2015,

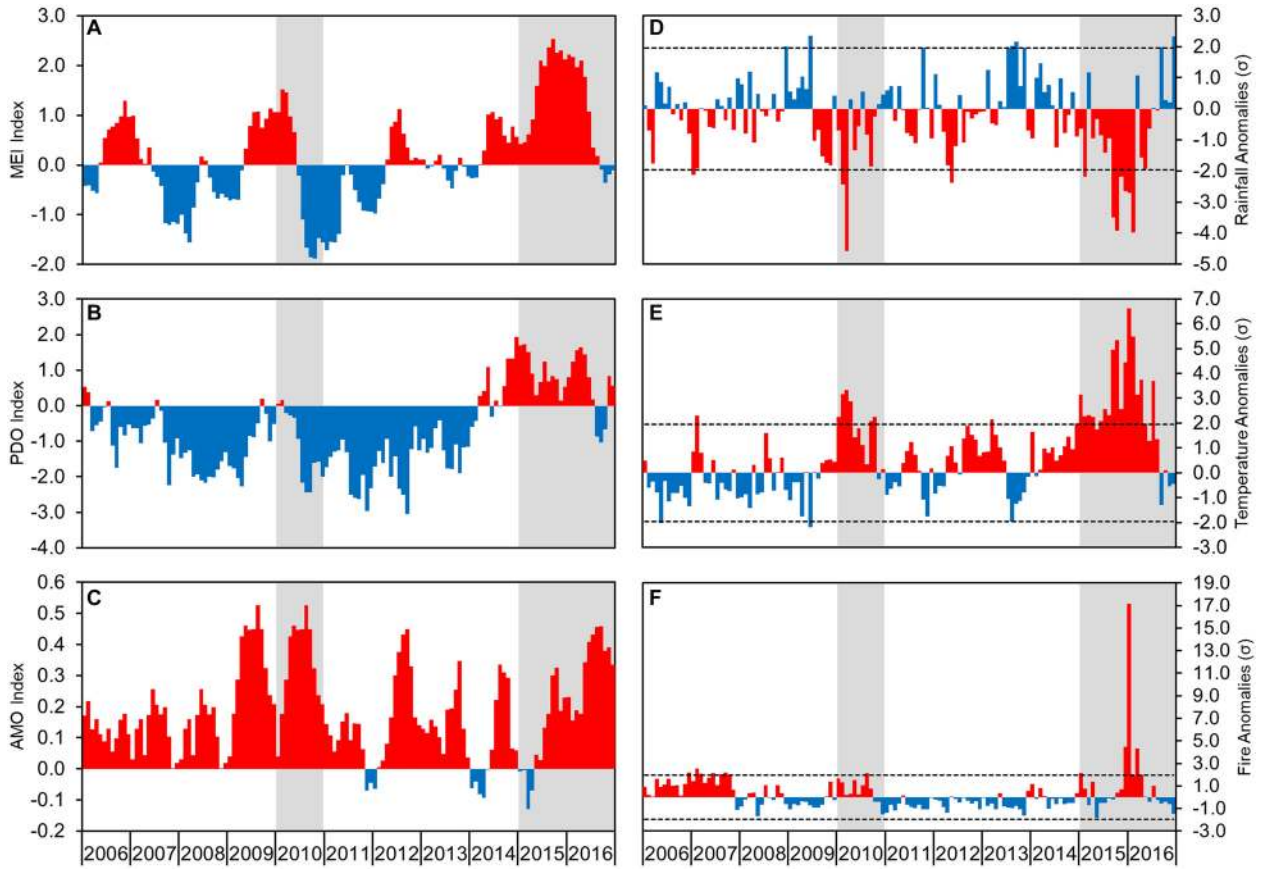

FIGURE 2 | Temporal pattern of oceanic indices and their influence on droughts, temperature and fires. Monthly anomalies of sea surface temperatures (SSTA) as measured by **(A)** the Multivariate El Niño index (MEI), **(B)** the Pacific Decadal Oscillation (PDO), **(C)** the Atlantic Multidecadal Oscillation (AMO). Rainfall (mm month^{-1}) **(D)** temperature (°C) **(E)** and **(F)** fire anomalies (count month^{-1}) were calculated based on a grid cell of 0.20° within the limits of the Brazilian Amazon biome. Red and blue bars indicate, respectively, positive and negative anomalies for all variables, except rainfall, which is displayed with reverse colors. Shaded areas indicate drought years here analyzed. The horizontal dashed lines represent the significant positive (blue bars) and negative anomalies (red bars). The absolute values of the rainfall, temperature, and fire monthly data are available in the **Supplementary Material**.

between Amazonas and Roraima states, representing about 4% (144,800 km^2) of the study area.

During JAS, which corresponds to the period where most of the study area is under the dry season, in 2010 and 2015 we observed large areas of significant negative rainfall anomalies, spatially concentrated in the central portion, at Amazonas and Pará states, corresponding to 8% (296,000 km^2) and 16% (561,600 km^2) of the total study area, respectively. In contrast, we identified a small area of significant negative rainfall anomalies in the southwest of Amazonas state in 2016, equivalent to 3% (98,800 km^2) of the total study area. Finally, we highlight the largest area of significant positive rainfall anomalies in the south region, representing 14% (508,400 km^2) of the total study area.

Concerning to the OND period, during the rainy season in most of the study area, we observed large areas of significant positive rainfall anomalies in 2010 and 2016 years, predominantly in the north region, corresponding to 9% (311,600 km^2) and 19% (686,800 km^2), respectively. Surprisingly, the largest area of significant negative rainfall anomalies, which was spatially generalized along the Brazilian Amazon biome, was identified in the JAS period of 2015, occupying an impressive 1,702,800 km^2 (47%) of the study area.

Temperature Anomalies

During the two analyzed droughts, there was a significant increase in the area affected by anomalous positive temperatures (**Figure 4**). During the period analyzed, the area affected by positive temperature anomalies exceeded the areas with negative anomalies, with exception of the last trimester of 2016.

During the 2010 drought, the significant positive temperature anomalies were observed mainly in JFM and AMJ periods, covering an area of 23% (840,400 km^2) and 21% (771,200 km^2), respectively, distributed along the whole Brazilian Amazon. Areas with significant positive temperature anomalies presented a decrease from 11% (404,400 km^2) to 9% (324,800 km^2) in the JAS and OND trimester, respectively. While in the JAS, the affected areas were concentrated mainly in the eastern and western fringes of the Brazilian Amazon biome. During OND, the positive anomalies were located in the south and west portions of the study area.

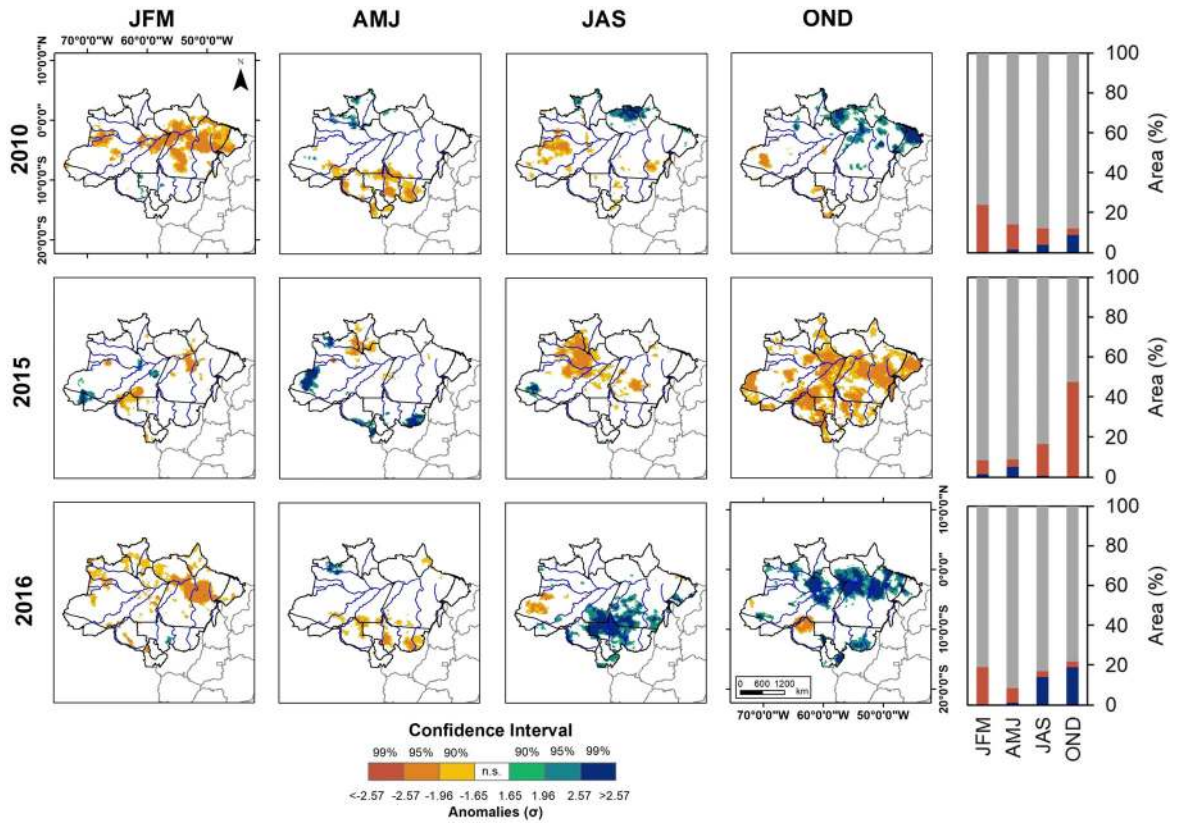

FIGURE 3 | Rainfall anomalies for the trimester periods in 2010, 2015, and 2016. The units are the anomalies normalized by the standard deviation (σ) of the time-series (2006–2016) for each 0.20° pixel. The right graphs show the proportional area (in relation to Brazilian Amazonian biome area) of significant rainfall anomalies ($p \leq 0.05$) for the same trimester period in 2010, 2015, and 2016.

Similarly, during the 2016 drought, significant positive temperature anomalies were identified mainly in the first 6 months. In the JFM period, the anomalies were distributed along the whole Brazilian Amazon biome, affecting more than half of the study area (51%, corresponding to 1,848,000 km^2). During the AMJ period, anomalous high temperatures were concentrated mainly in the central and east region, representing 24% (875,200 km^2) of the study area. From July to December, the area affected by high temperatures started to decrease, from 15% (542,400 km^2) to 2% (74,000 km^2), scattered throughout the study area. In contrast, during the 2015 drought, significant positive temperature anomalies occurred along the whole Brazilian Amazon biome for all the analyzed trimesters. Differently from 2010 and 2016 droughts, the largest areas affected by anomalous high temperature in 2015 occurred in the second semester of the year, during the JAS period, covering 51% (1,821,600 km^2), and in OND period, with an extent of 2,188,800 km^2, 61% of the study area.

Fire Anomalies

Figure 5 shows the spatial pattern of active fire anomalies calculated for each three-monthly period for the 2010, 2015, and 2016 drought years. In general, areas with negative significant fire anomalies, which corresponds to less active fire pixels than the average, affected less than 1% of the study area.

In the three analyzed years (2010, 2015, and 2016), positive fire anomalies were evident in the north of the studied region in the JFM trimester, shifting to the south in the AMJ trimester, and spreading across the study area in JAS trimester. Following this period, the area impacted decreased, with a mix of positive and negative anomalies in the west and south of the study area. During JAS trimester of 2010, we observed a peak in affected area totalizing 7.8% (278,800 km^2), followed by the OND period in 2015, with 6.4% (231,200 km^2) of the study area. In 2016 during JFM trimester, the peak in area affected by fires reached 2% (75,600 km^2) of the study area. On the other hand, during the AMJ period, positive fire anomalies were detected in the south region of Amazonia but represented an area smaller than 1% of the study region. Surprisingly, during the 2015 and 2016 years, in the JFM and OND trimester periods, the positive fire anomalies extended beyond the Arc of Deforestation, scattered in the central and north regions.

The combination of decreased rainfall and increased temperature made the landscape more susceptible to fire in Amazonia. **Figure 6** shows the proportion of pixels with significant positive fire anomalies ($p \leq 0.05$) associated with

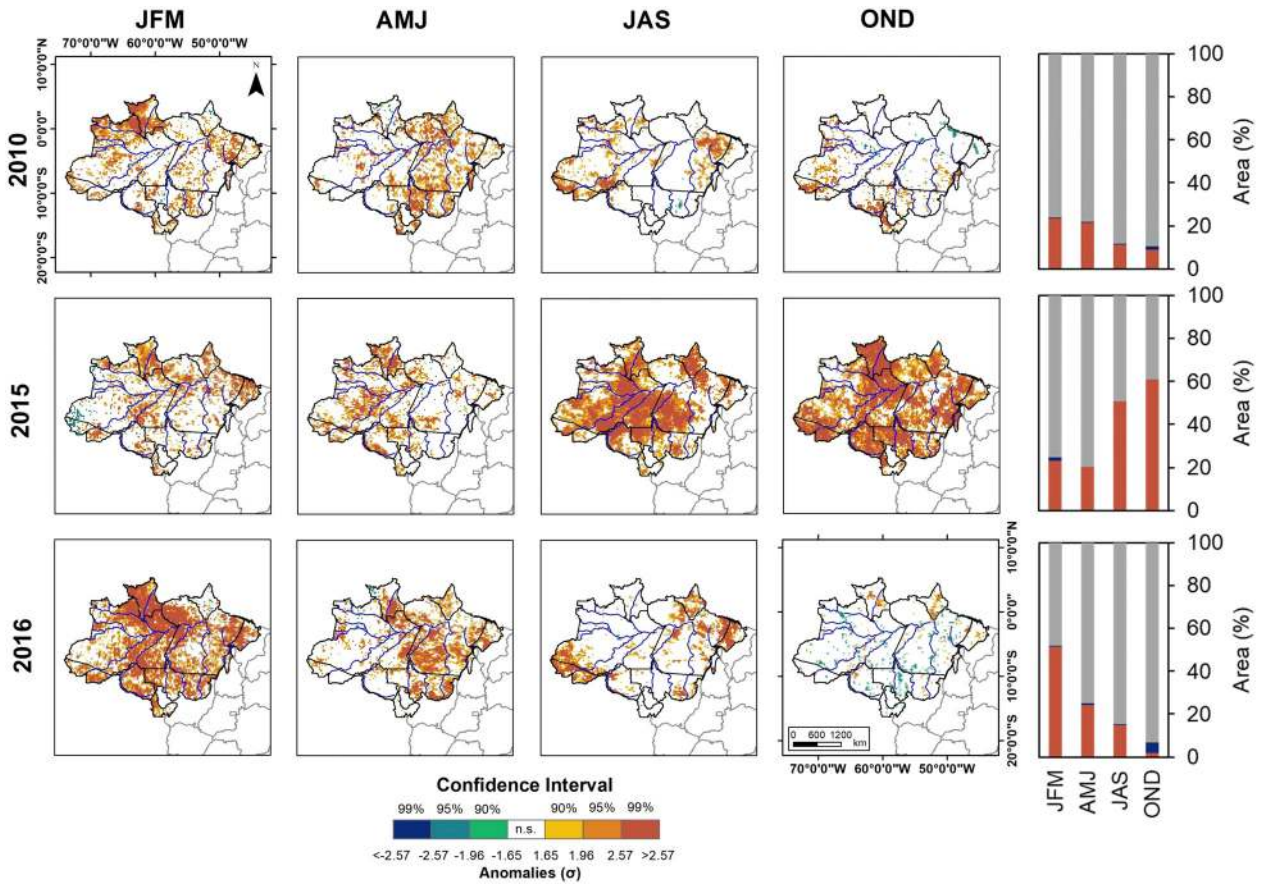

FIGURE 4 | Land surface temperature anomalies for the trimester periods in 2010, 2015, and 2016. The units are the anomalies normalized by the standard deviation (σ) of the time-series (2006–2016) for each 0.20° pixel. The right graphs show proportional area (in relation to Brazilian Amazonian biome area) of significant temperature anomalies ($p \leq 0.05$) for the same trimester period in 2010, 2015, and 2016.

rainfall decrease, temperature increase or both. Throughout the analyzed droughts, we observed that the significant positive fire anomalies interacted with rainfall reduction, temperature increase or both. These interactions differed among the two droughts. During the first semester of 2010, more than half of the pixels with significant positive fire anomalies (66% in the JFM and 62% in the AMJ) were associated with anomalous rainfall reduction and temperature increase. On the other hand, in the last two trimesters of 2010, the grid cells proportion ranged from 21% in the JAS to 25% in the OND trimester. During the 2015 drought, we observed an inverse pattern, with significant positive fire anomalies pixels associated with rainfall reduction and temperature increase ranged from 15% in the AMJ period to 49% in the JFM, and from 64% in the JAS to 86% in the OND trimester. However, during the 2016 drought, the proportion of pixels with significant positive fire anomalies associated with rainfall reduction and temperature increase progressively decreased from the beginning to the end of the year, from 87% in the JFM to 9% in the OND. Overall, temperature anomalies contributed significantly to the increase of fires during the 2015 and 2016 droughts. However, the interaction between rainfall reduction and temperature increase dominated the last trimester of 2015 and the first trimester of 2016.

Recurrence of the Rainfall, Temperature, and Fire Anomalies

The recurrence of significantly anomalous low rainfall and high temperatures, both affected extensive areas during the end of wet season and beginning of the dry season (JFM and AMJ trimester) (**Figure 7**). Areas affected by significant negative anomalies represent more than 20% of the study area, in each trimester, while the areas affected by significant positive anomalies were larger than 25% of the study area. Spatially, however, the patterns were distinct. While areas affected two or three times with abnormally low rainfall were located in the eastern and southern parts of Amazonia (**Figure 7**; first row), anomalous high temperature recurrence was concentrated in the northern part of the study area (**Figure 7**; second row). The two-time recurrence of positive fire anomalies varied between 10 and 19%, of the area peaking when most of the region was under the wet season. The largest areas with anomalies in JFM were located in the northern part of the Amazon, which during this period is under the dry

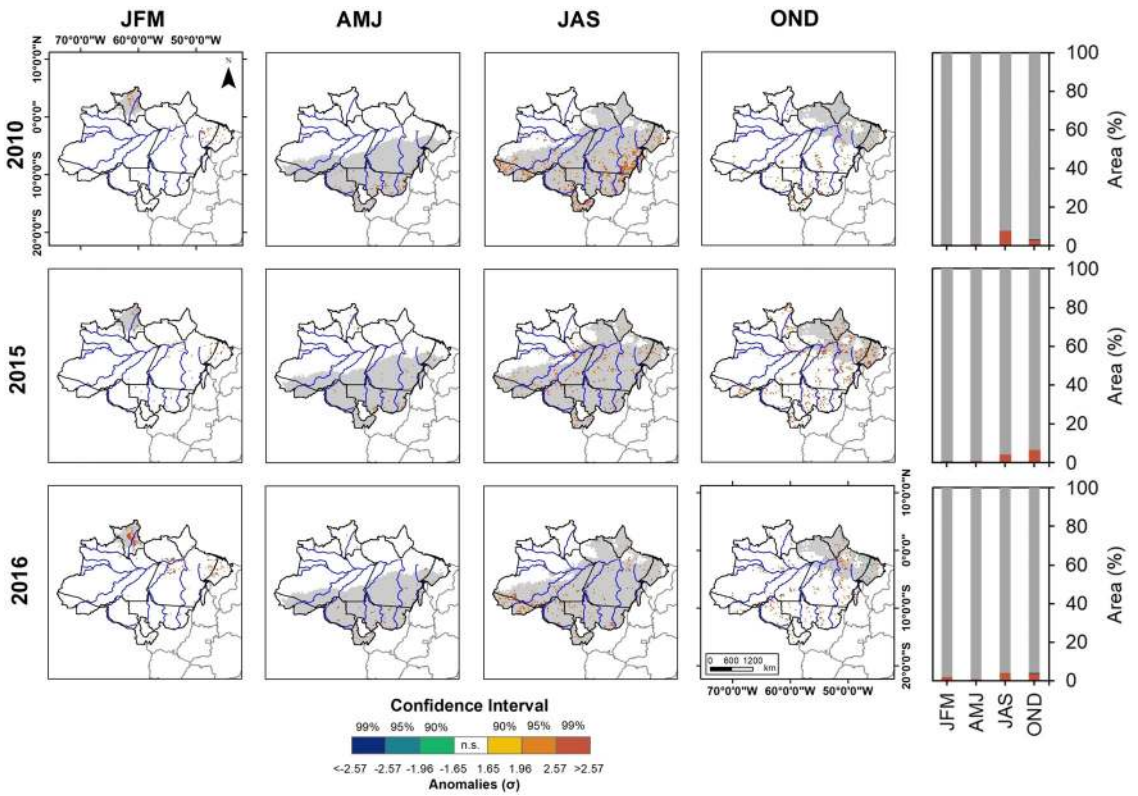

FIGURE 5 | Active fire anomalies for the trimester period in 2010, 2015, and 2016. The units are the anomalies normalized by the standard deviation (σ) of the time-series (2006–2016) for each 0.20° pixel. The right graphs show proportional area (in relation to Brazilian Amazonian biome area) of significant active fire anomalies ($p \leq 0.05$) for the same trimester period in 2010, 2015, and 2016. The gray background in the maps represents areas that were under dry season based on a rainfall threshold of 100 mm month^{-1} (Moura et al., 2015).

season. Interestingly, during OND, areas which are under the wet season also exhibited positive fire anomalies, including the central region, along the margins of the Amazon river (**Figure 7**; third row).

Burned Area by Land Use and Land Cover and Fire-Associated Carbon Dioxide Emissions

Figure 8A shows burned areas and their respective annual proportions classified by different types of land use and land cover within Brazilian Amazon biome. In 2007, we observed the largest total annual burned area (41,919 km^2), were 69% occurred in productive lands, 17% in non-forest vegetation, and 14% in forest cover. On the other hand, 2013 had the lowest annual burned area (9,132 km^2) were 54% occurred in productive lands, 28% in non-forest vegetation, and 18% in forest cover.

A total of 41,378 km^2 of burned area was observed during the 2010 Amazonian drought (**Figure 8A**), dominated by productive land fires (68%; 28,161 km^2), with 12% (5,032 km^2) of fires occurring in forested areas. During the same drought, we observed a simultaneous burned area increase of 168% in productive land (**Figure 8D**), 73% in non-forest vegetation (**Figure 8C**) and 91% in forest covers (**Figure 8**).

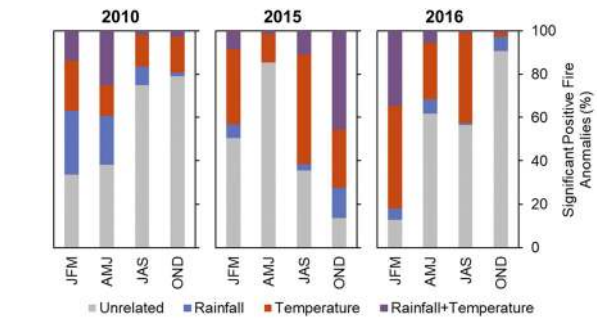

FIGURE 6 | Significant positive fire anomalies ($p \leq 0.05$) classified by rainfall and temperature interactions in the four trimesters of 2010, 2015, and 2016. Rainfall Class: pixels with significant positive fire anomaly and significant negative rainfall anomaly. Temperature Class: pixels with significant positive fire anomaly and significant positive temperature anomaly.
Rainfall + Temperature Class: pixels with significant positive fire anomaly and significant negative rainfall anomaly plus significant positive temperature anomaly. Unrelated Class: other combinations.

Remarkably contrasting, the 2015/2016 Amazonian drought had 20,049 km^2 of burned area in 2015 and 16,994 km^2 in 2016 (**Figure 8A**), with 55% (10,944 km^2)

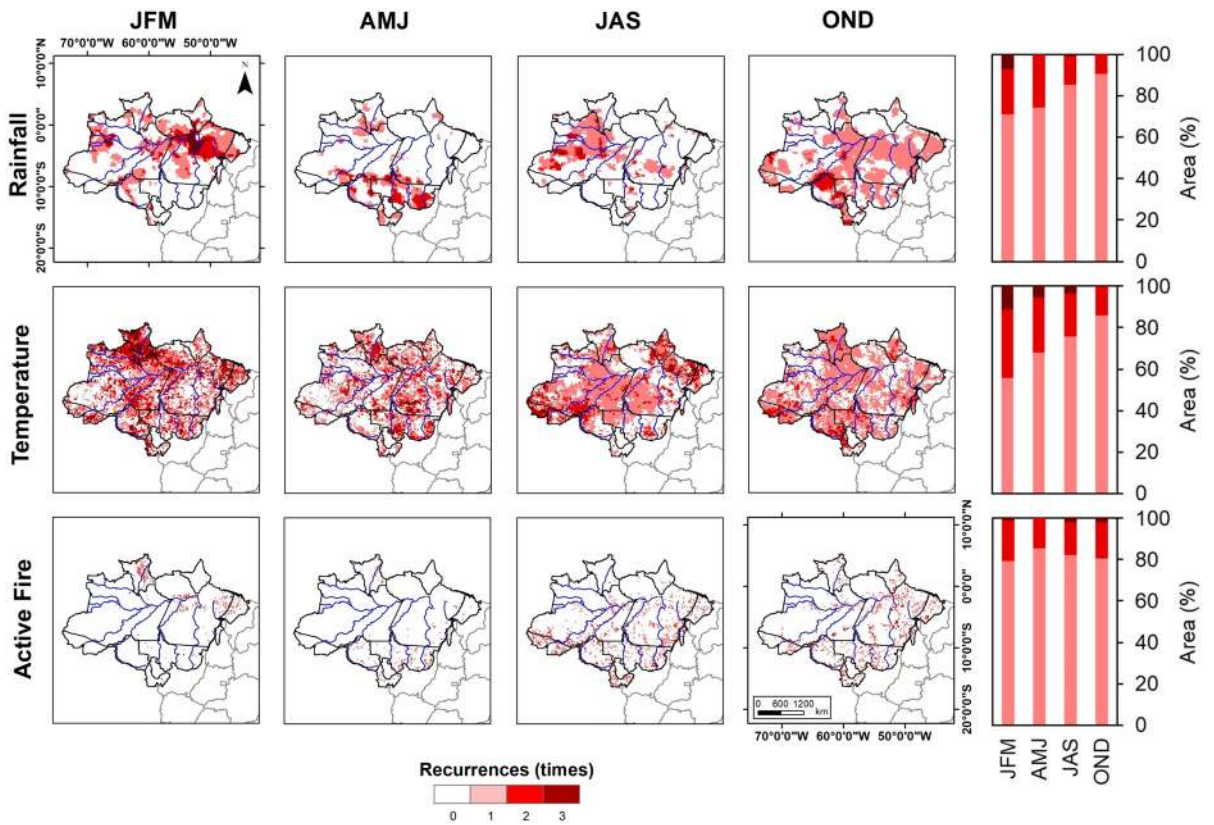

FIGURE 7 | Recurrence of significant negative anomalies of rainfall and positive anomalies of temperature and fire per trimester during the 2010, 2015, and 2016 droughts. The right graphs show proportional area (in relation to Brazilian Amazonian biome area) of significant active fire anomalies ($p \leq 0.05$) for the same trimester period in 2010, 2015, and 2016.

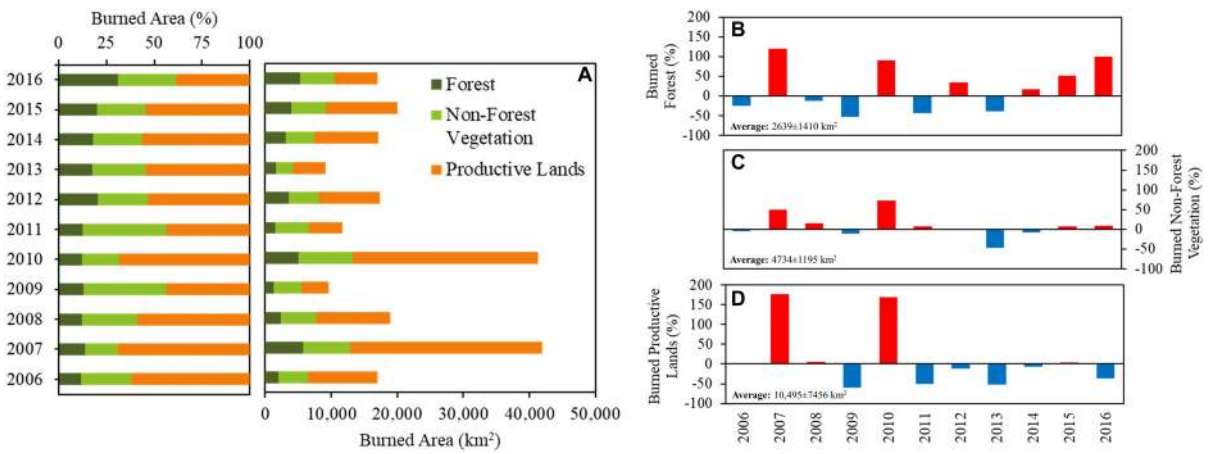

FIGURE 8 | (A) Burned area by land use and land cover. **(B)** Difference as percentage between the annual burned area in forests and the average (2006–2016) excluding drought years. **(C)** Difference as percentage between the annual burned area in non-forest vegetation and the average (2006–2016) excluding drought years. **(D)** Difference as percentage between the annual burned area in productive lands and the average (2006–2016) excluding drought years.

and 39% (6,568 km^2) of productive lands fires in 2015 and 2016, respectively. Surprisingly, during the same drought, burned forests corresponded to 20% (3,993 km^2) and 31% (5,253 km^2) in 2015 and 2016, respectively, surpassing the other analyzed years. We also highlight that, unlike the 2010 Amazonian drought, during the 2015/2016 drought, we observed a simultaneous burned forest increase of 51% and 99% (**Figure 8B**) in 2015 and 2016,

respectively, while burned non-forest vegetation increased only 8% in 2015 and 9% in 2016 (**Figure 8C**), and burned productive lands increase 4% in 2015 and decrease 37% in 2016. These results reinforce the dominance of wildfires during the 2015/2016 drought in the Brazilian Amazon biome.

Fires in natural and anthropic environments result in the emission of particulates and gases. In **Figure 9**, we show the seasonality, anomalies and total carbon dioxide (CO_2) emission within Brazilian Amazon biome. In general, the lowest monthly CO_2 emissions were present in January and February for all analyzed years, with peaks of emission mainly in August and September (**Figure 9A**). However, in 2010 we found significant ($p \leq 0.05$) monthly CO_2 increases revealed by five positive anomalies in January (2.00 σ), February (2.47 σ), April (3.29 σ), July (2.06 σ), and August (3.47 σ), while no significant negative anomalies were observed (**Figure 9B**). On the other hand, in 2015 and 2016, four significant positive anomalies ($p \leq 0.05$) were identified for each of the years, without significant negative anomalies (**Figure 9B**). Although with a smaller number of significant positive anomalies, the 2015/2016 Amazonian drought was characterized by extremely high positive anomalies of CO_2, for example, the anomaly of 11.23 σ in December 2015 and 34.46 σ in January 2016 (**Figure 9B**).

In the annual scale, the year 2007 had the highest accumulated CO_2 emission, totalizing 264 Tg, while the year of 2011 had the lowest, totalizing 38 Tg. During the 2010 Amazonian drought, 233 Tg CO_2 were emitted to atmosphere, while the 2015/2016 Amazonian drought emitted 242 Tg CO_2, being 147 Tg CO_2 (61%) in 2015 and 95 Tg CO_2 (39%) in 2016. In addition, we found that CO_2 emissions during the last trimester of 2015 (OND) and the first of 2016 (JFM) exceeded by 295% and 369%, respectively, the average of previous years.

DISCUSSION AND CONCLUSION

Causes and Spatio-Temporal Patterns of the 2010 and 2015/2016 Amazonian Droughts

Commonly, the spatial and temporal natural variability of rainfall in Amazonia can be influenced by El Niño/La Niña events or by temperature anomalies in the Tropical North Atlantic. Our results showed that the 2010 drought was related to the warming of the North Atlantic Ocean, measured by the AMO Index, while the 2015/2016 drought, significant rainfall reduction was induced by an anomalous warming of both the Atlantic and Pacific ocean, as evidenced by the AMO, MEI, and PDO indices (Schlesinger and Ramankutty, 1994; Mantua et al., 1997; Enfield et al., 2001; Wolter and Timlin, 2011). This results corroborate previous findings for the Amazonia (Lewis et al., 2011; Marengo et al., 2011; Saatchi et al., 2013; Aragão et al., 2018). In contrast, the 2016 drought occurred under a cooling of the Pacific Ocean, revealed by a progressive reduction of PDO and MEI indices, but with a steady warming of the North Atlantic, as evidenced by the AMO index. The surface warming in different oceans causes changes in large-scale atmospheric circulation patterns, mainly associated with the Hadley Cell and Walker Circulation, resulting in significantly below-average rainfall over Amazonia (McGregor et al., 2014; Aragão et al., 2018; Barichivich et al., 2018).

Spatially, sea surface warming affects heterogeneously the patterns of rainfall along the Brazilian Amazon. Positive anomalies in the AMO index reduce rainfall in the southwest region, while positive MEI and PDO index reduce rainfall in the central and northern regions of the Brazilian Amazon (Aragão et al., 2018). These relationships explain the spatial patterns and extent of negative rainfall anomalies observed here for the two droughts analyzed, especially in the last trimester of 2015 and the first of 2016, resulting from the simultaneous warming of the Atlantic and Pacific Oceans.

We also highlight the occurrence of significant negative rainfall anomalies during the wet season, specifically between January and April 2010, and between October 2015 and March 2016. These findings are consistent with the trend of increase in the dry season length of the Amazonia, observed since 1983 (Marengo et al., 2018).

Here, our findings revealed a significant warming of the Brazilian Amazon surface during the 2010 and 2015/2016 droughts. At the monthly scale, the 2015/2016 drought was accompanied by a strong and successive positive surface temperature anomaly, while during the 2010 drought, positive anomalies of surface temperature were less intense, showing a cooling trend toward the month of December. At the three-monthly time scale, the magnitude of surface warming was repeated spatially, since more than half of the Brazilian Amazon experienced significant positive temperature anomalies, during the last two trimesters of 2015 and first of 2016, corroborating and adding to the results presented by Jiménez-Muñoz et al. (2016). This anomalous surface warming can be explained by an increase in the direct solar radiation reaching the land surface (Anderson et al., 2010), resulting from a drastic reduction in cloud cover during extreme droughts in Amazonia (Jimenez et al., 2018; Martins et al., 2018). According to Jiménez-Muñoz et al. (2016), anomalous surface warming combined with reduced rainfall can increase drought severity by 20% in the Amazon, due to the increase in potential evapotranspiration.

In Amazonia, changes in the rainfall regime, especially in the dry season, is one of the main concerns in a world exposed to climatic changes (Malhi et al., 2008). Model projections (Li et al., 2006; Malhi et al., 2008; Duffy et al., 2015) pointed to a drier climate with more frequent extreme droughts for Amazonia, corroborating with our findings. Besides, the global warming effect tend to be intensified during El Niño events (Cai et al., 2018), which based on our findings, may cause more frequent and intense droughts in the Brazilian Amazon biome (Duffy et al., 2015).

Spatio-Temporal Response of Fire Occurrence During the 2010 and 2015/2016 Amazonian Droughts

In Amazonia, anomalous fire occurrence is related to the synergy among drought events, forest fragmentation, and ignition sources (Aragão et al., 2007, 2018; Aragão and Shimabukuro, 2010;

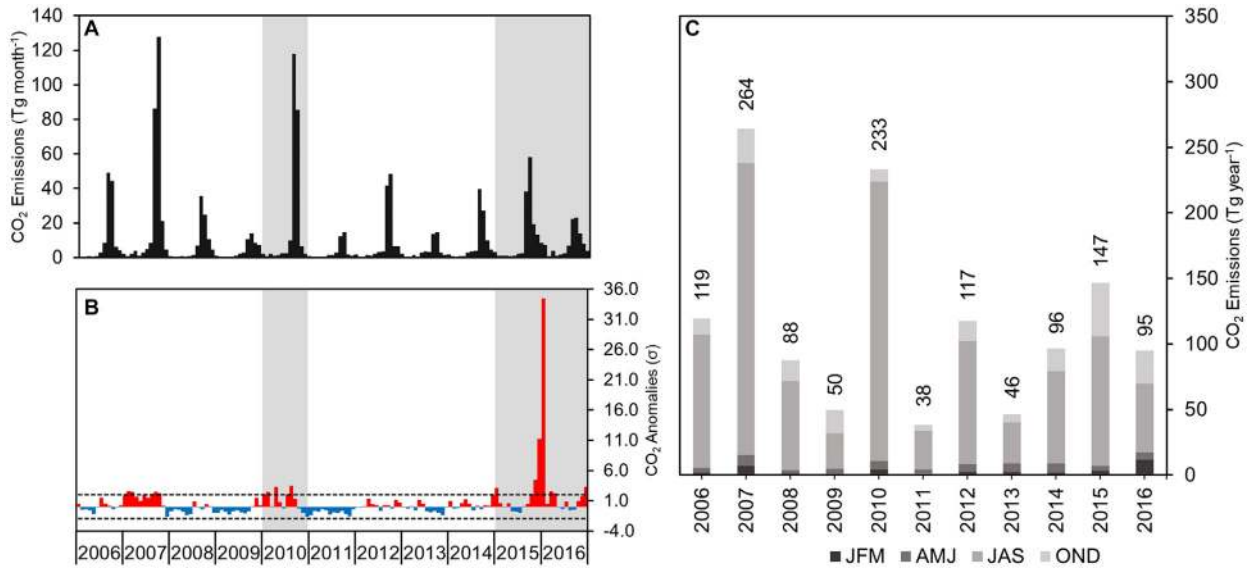

FIGURE 9 | Carbon dioxide (CO_2) emissions between 2006 and 2016 estimated for the Brazilian Amazon from the Global Fire Emissions Database (GFEDv4). **(A)** Seasonal pattern of CO_2 emissions. **(B)** Monthly anomalies of CO_2 emissions. **(C)** Total CO_2 emissions by year and trimester.

Armenteras et al., 2013, 2017; Cano-Crespo et al., 2015; Silva Junior et al., 2018b). Here, we clearly show the association between active fires and rainfall in the monthly and trimestral scale, corroborating previous studies (Aragão et al., 2007, 2018). During the 2015/2016 drought, moreover, we demonstrated the interaction between negative rainfall and positive temperature anomalies that resulted in large positive fire anomalies from late 2015 to early 2016. Interestingly, the increase in fire occurred outside the usual fire season, from June to October in most of the region (Anderson et al., 2015). Our results indicated large areas of significant positive fire anomalies during the OND trimester in 2015 and 2016. Unlike the 2010 drought, in the 2015/2016 drought, positive fire anomalies were observed beyond the Arc of Deforestation, mainly in Roraima, Amazonas and Pará states.

Different from the 2010 drought, during the 2015/2016 drought, positive anomalies of active fires were accompanied by the highest negative rainfall and positive temperature anomalies, in the last trimester of 2015 and the first of 2016. This configuration was also observed in the spatial analyses, were more than 65% of cells with significant fires anomalies were related to significant temperature anomalies. The higher contribution of temperature explained the extent and magnitude of anomalous fires occurrence observed during the 2015/2016 drought, corroborating recent findings which showed evidences that temperature may be an important driver of active fires incidence in Amazonia (Lima et al., 2018). In addition, by evaluating annual patterns of rainfall, temperature and fire anomalies we show a clear spatial pattern of fires following areas with high temperature and low rainfall during the two droughts analyzed (**Supplementary Figure 1**).

In Amazonia, vegetation is sensitive to variation in rainfall patterns (Phillips et al., 2009; Hilker et al., 2014; Anderson et al., 2018), where droughts make forests drier and hotter, increasing their susceptibility to fire (Nepstad et al., 2004). Moreover, during droughts, fuel loads tend to increase in the forest understory, as a consequence of increased tree mortality (Nepstad et al., 2007; Brando et al., 2008; Brienen et al., 2015). During the 2010 drought, fire anomalies were associated to the simultaneous increase of fires occurring in forests, non-forest vegetation and productive lands. However, during the 2015/2016 drought, fire anomalies had a large contribution from fires occurring in forested areas (**Supplementary Figure 2**).

Natural forest fires are considered rare in Amazonia (Cochrane, 2003; Bush et al., 2007), however, with the increase in the occurrence and intensification of droughts, forest fragmentation and abundance of anthropic ignition sources, fire becomes prone to escape from open areas into adjacent forest edges, spreading progressively toward the forest interior (Cano-Crespo et al., 2015; Silva Junior et al., 2018b). Differently from 2010, during the 2015/2016 drought, water deficit in the northern region of the Brazilian Amazon increased substantially, varying between 392 and 2,086 mm (**Supplementary Figure 3**), which led to a widespread occurrence of forest fires in the same period. During the 2015/2016 drought, forest fire patterns are likely to be associated with different ignition sources. In the extreme north of the Amazonia, in the state of Roraima, sources of ignition were dominated by traditional subsistence practices (Fonseca et al., 2017). In Amazonas and Pará, contrarily, most forest fires occurred adjacent to agricultural and livestock farms (Withey et al., 2018). Moreover, in Maranhão state, most of the forest fires were of criminal origin, ignited by loggers in the region called "Mosaico Gurupi" (Celentano et al., 2017a,b), which is composed by protected areas and indigenous lands.

Based on our findings, we anticipate the increase and dominance of forest fires in the Brazilian Amazon biome during extreme droughts, which may result in large amounts of carbon

dioxide emissions into the atmosphere, affecting the stability of the regional and global carbon cycle.

Fire-Associated Carbon Dioxide (CO_2) Emissions During the 2010 and 2015/2016 Amazonian Droughts

Our analysis shows that drought-induced fires increase carbon dioxide (CO_2) emissions to the atmosphere in Amazonia at a monthly scale, evidenced by significant positive anomalies. Although total CO_2 emissions during the 2010 drought (233 Tg C) were higher than the annual emissions in 2015 (147 Tg C) and 2016 (95 Tg C), emissions in the last trimester of 2015 and the first of 2016 were overwhelmingly anomalous. Interestingly, these two trimesters usually correspond to the wet season, where the occurrence of fires are minimal in Amazonia (Aragão et al., 2008).

In Brazil, the National Plan on Climate Change was defined through Federal Decree No. 6263 of 21 November 2008 (NPCC-Interministerial Committee on Climate Change, 2008). This document established national targets for reducing deforestation rates below a baseline of the average deforestation from 1996 to 2005, representing a decrease of 1.3 Pg CO_2 in emissions to the atmosphere from 2006 to 2017, about 0.11 Pg CO_2 year^{-1}. The total CO_2 emissions quantified here using GFEDv4 for the Brazilian Amazon in 2010 (0.23 Pg CO_2), 2015 (0.15 Pg CO_2), and 2016 (0.09 Pg CO_2), represents, respectively, 209%, 136%, and 82% of annual Brazil's national target.

Finally, we suggest that drought-induced fire emissions should be included in policies for reducing greenhouse gases emissions, as well as regulations on fire use to prevent the escape of fire to adjacent forests during dry years.

AUTHOR CONTRIBUTIONS

CSJ, LOA, and LEA contributed to the conception and design of the study. AS, CA, RD, and RP organized and processed the dataset. CSJ performed the statistical analysis. CSJ, LOA, AS, CA, MP, TP, and LEA wrote the manuscript. All authors contributed to the manuscript revision and approved the submitted version.

FUNDING

This study was financed in part by the Coordenação de Aperfeiçoamento de Pessoal de Nível Superior – Brasil (CAPES) – Finance Code 001, the National Council for Scientific and Technological Development – CNPq (Grants Nos. 309247/2016-0, 305054/2016-3, 140502/2016-5, and 140377/2018-2), and São Paulo Research Foundation – FAPESP (Grants Nos. 2015/22987-7, 16/02018-2, and 2017/15257-8). The funders had no role in study design, data collection and analysis, decision to publish, or preparation of the manuscript.

ACKNOWLEDGMENTS

We thank the scientists at the National Oceanic and Atmospheric Administration – NOAA, the Climate Hazards Group – CHG, the National Aeronautics and Space Administration – NASA, and the MapBiomas Project for providing the freely available datasets. Finally, we also thank the editor and reviewers whose helpful comments and suggestions helped to improve and clarify this manuscript.

SUPPLEMENTARY MATERIAL

The Supplementary Material for this article can be found online at: https://www.frontiersin.org/articles/10.3389/feart.2019.00097/full#supplementary-material

REFERENCES

Akagi, S. K., Yokelson, R. J., Wiedinmyer, C., Alvarado, M. J., Reid, J. S., Karl, T., et al. (2011). Emission factors for open and domestic biomass burning for use in atmospheric models. *Atmos. Chem. Phys.* 11, 4039–4072. doi: 10.5194/acp-11-4039-2011

Alvares, C. A., Stape, J. L., Sentelhas, P. C., de Moraes Gonçalves, J. L., and Sparovek, G. (2013). Köppen's climate classification map for Brazil. *Meteorol. Zeitschrift* 22, 711–728. doi: 10.1127/0941-2948/2013/0507

Anderson, L. O. (2012). Biome-scale forest properties in amazonia based on field and satellite observations. *Remote Sens.* 4, 1245–1271. doi: 10.3390/rs4051245

Anderson, L. O., Aragão, L. E., Gloor, M., Arai, E., Adami, M., Saatchi, S. S., et al. (2015). Disentangling the contribution of multiple land covers to fire-mediated carbon emissions in amazonia during the 2010 drought. *Global Biogeochem. Cycles* 29, 1739–1753. doi: 10.1002/2014GB005008

Anderson, L. O., Malhi, Y., Aragão, L. E., Ladle, R., Arai, E., Barbier, N., et al. (2010). Remote sensing detection of droughts in Amazonian forest canopies. *New Phytol.* 187, 733–750. doi: 10.1111/j.1469-8137.2010.03355.x

Anderson, L. O., Ribeiro Neto, G., Cunha, A. P., Fonseca, M. G., Mendes de Moura, Y., Dalagnol, R., et al. (2018). Vulnerability of Amazonian forests to repeated droughts. *Philos. Trans. R. Soc. B Biol. Sci.* 373:20170411. doi: 10.1098/rstb.2017.0411

Anderson, L. O., Trivedi, M., Queiroz, J., Aragão, L., Marengo, J. A., Young, C., et al. (2011). "Counting the costs of the 2005 amazon drought: a preliminary assessment," in *Ecosystem Services for Poverty Alleviation in Amazonia*, ed. P. Meir (Edinburgh: Global Canopy Programme and Univ. of Edinburgh), 96–108.

Andreae, M. O., and Merlet, P. (2001). Emission of trace gases and aerosols from biomass burning. *Global Biogeochem. Cycles* 15, 955–966. doi: 10.1029/2000GB001382

Aragão, L. E., Malhi, Y., Barbier, N., Lima, A. A., Shimabukuro, Y., Anderson, L., et al. (2008). Interactions between rainfall, deforestation and fires during recent years in the Brazilian Amazonia. *Philos. Trans. R. Soc. Lond. B. Biol. Sci.* 363, 1779–1785. doi: 10.1098/rstb.2007.0026

Aragão, L. E., Malhi, Y., Roman-Cuesta, R. M., Saatchi, S., Anderson, L. O., and Shimabukuro, Y. E. (2007). Spatial patterns and fire response of recent Amazonian droughts. *Geophys. Res. Lett.* 34:L07701. doi: 10.1029/2006GL028946

Aragão, L. E., Poulter, B., Barlow, J. B., Anderson, L. O., Malhi, Y., Saatchi, S., et al. (2014). Environmental change and the carbon balance of Amazonian forests. *Biol. Rev.* 89, 913–931. doi: 10.1111/brv.12088

Aragão, L. E., and Shimabukuro, Y. E. (2010). The incidence of fire in Amazonian forests with implications for REDD. *Science* 328, 1275–1278. doi: 10.1126/science.1186925

Aragão, L. E. O. C., Anderson, L. O., Fonseca, M. G., Rosan, T. M., Vedovato, L. B., Wagner, F. H., et al. (2018). 21st Century drought-related fires counteract the decline of Amazon deforestation carbon emissions. *Nat. Commun.* 9:536. doi: 10.1038/s41467-017-02771-y

Armenteras, D., Barreto, J. S., Tabor, K., Molowny-Horas, R., and Retana, J. (2017). Changing patterns of fire occurrence in proximity to forest edges, roads and rivers between NW Amazonian countries. *Biogeosciences* 14, 2755–2765. doi: 10.5194/bg-14-2755-2017

Armenteras, D., González, T. M., and Retana, J. (2013). Forest fragmentation and edge influence on fire occurrence and intensity under different management types in Amazon forests. *Biol. Conserv.* 159, 73–79. doi: 10.1016/j.biocon.2012.10.026

Barichivich, J., Gloor, E., Peylin, P., Brienen, R. J. W., Schöngart, J., Espinoza, J. C., et al. (2018). Recent intensification of Amazon flooding extremes driven by strengthened walker circulation. *Sci. Adv.* 4:eaat8785. doi: 10.1126/sciadv.aat8785

Brando, P. M., Nepstad, D. C., Davidson, E. A., Trumbore, S. E., Ray, D., and Camargo, P. (2008). Drought effects on litterfall, wood production and belowground carbon cycling in an Amazon forest: results of a throughfall reduction experiment. *Philos. Trans. R. Soc. B Biol. Sci.* 363, 1839–1848. doi: 10.1098/rstb.2007.0031

Brienen, R. J. W., Phillips, O. L., Feldpausch, T. R., Gloor, E., Baker, T. R., Lloyd, J., et al. (2015). Long-term decline of the Amazon carbon sink. *Nature* 519, 344–348. doi: 10.1038/nature14283

Bush, M. B., Silman, M. R., de Toledo, M. B., Listopad, C., Gosling, W. D., Williams, C., et al. (2007). Holocene fire and occupation in Amazonia: records from two lake districts. *Philos. Trans. R. Soc. B Biol. Sci.* 362, 209–218. doi: 10.1098/rstb.2006.1980

Cai, W., Wang, G., Dewitte, B., Wu, L., Santoso, A., Takahashi, K., et al. (2018). Increased variability of eastern Pacific El Niño under greenhouse warming. *Nature* 564, 201–206. doi: 10.1038/s41586-018-0776-9

Campanharo, W., Lopes, A., Anderson, L., da Silva, T., and Aragão, L. (2019). Translating fire impacts in southwestern amazonia into economic costs. *Remote Sens.* 11:764. doi: 10.3390/rs11070764

Cano-Crespo, A., Oliveira, P. J. C., Boit, A., Cardoso, M., and Thonicke, K. (2015). Forest edge burning in the Brazilian Amazon promoted by escaping fires from managed pastures. *J. Geophys. Res. Biogeosci.* 120, 2095–2107. doi: 10.1002/2015JG002914

Cano-Crespo, A., Oliveira, P. J. C., Cardoso, M., and Thonicke, K. (2014). "Tropical forest degradation in the Brazilian Amazon: relation to fire and land-use change," in *Advances in Forest Fire Research*, (Coimbra: Imprensa da Universidade de Coimbra), 1582–1591. doi: 10.14195/978-989-26-0884-6_174

Celentano, D., Miranda, M. V. C., Rousseau, G. X., Muniz, F. H., Loch, V., do, C., et al. (2017a). Desmatamento, degradação e violência no "Mosaico Gurupi" – A região mais ameaçada da Amazônia. *Estud. Avançados* 32, 315–339. doi: 10.5935/0103-4014.20180021

Celentano, D., Rousseau, G. X., Muniz, F. H., Varga, I., van, D., Martinez, C., et al. (2017b). Towards zero deforestation and forest restoration in the Amazon region of Maranhão state, Brazil. *Land Use Policy* 68, 692–698. doi: 10.1016/j.landusepol.2017.07.041

Chuvieco, E., Lizundia-Loiola, J., Pettinari, M. L., Ramo, R., Padilla, M., Tansey, K., et al. (2018). Generation and analysis of a new global burned area product based on MODIS 250 m reflectance bands and thermal anomalies. *Earth Syst. Sci. Data* 10, 2015–2031. doi: 10.5194/essd-10-2015-2018

Cochrane, M. A. (2003). Fire science for rainforests. *Nature* 421, 913–919. doi: 10.1038/nature01437

Cochrane, M. A., and Laurance, W. F. (2008). Synergisms among fire, land use, and climate change in the amazon. *AMBIO A J. Hum. Environ.* 37, 522–527. doi: 10.1579/0044-7447-37.7.522

Coelho, C. A. S., Cavalcanti, I. A. F., Costa, S. M. S., Freitas, S. R., Ito, E. R., Luz, G., et al. (2012). Climate diagnostics of three major drought events in the Amazon and illustrations of their seasonal precipitation predictions. *Meteorol. Appl.* 19, 237–255. doi: 10.1002/met.1324

Correa, S. W., de Paiva, R. C. D., Espinoza, J. C., and Collischonn, W. (2017). Multi-decadal hydrological retrospective: case study of amazon floods and droughts. *J. Hydrol.* 549, 667–684. doi: 10.1016/j.jhydrol.2017.04.019

Duan, Z., Liu, J., Tuo, Y., Chiogna, G., and Disse, M. (2016). Evaluation of eight high spatial resolution gridded precipitation products in Adige Basin (Italy) at multiple temporal and spatial scales. *Sci. Total Environ.* 573, 1536–1553. doi: 10.1016/j.scitotenv.2016.08.213

Duffy, P. B., Brando, P., Asner, G. P., and Field, C. B. (2015). Projections of future meteorological drought and wet periods in the Amazon. *Proc. Natl. Acad. Sci. U.S.A.* 112, 13172–13177. doi: 10.1073/pnas.1421010112

Enfield, D. B., Mestas-Nuñez, A. M., and Trimble, P. J. (2001). The atlantic multidecadal oscillation and its relation to rainfall and river flows in the continental U.S. *Geophys. Res. Lett.* 28, 2077–2080. doi: 10.1029/2000GL012745

Fanin, T., and van der Werf, G. R. (2015). Relationships between burned area, forest cover loss, and land cover change in the Brazilian Amazon based on satellite data. *Biogeosciences* 12, 6033–6043. doi: 10.5194/bg-12-6033-2015

Fearnside, P. M. (2005). Deforestation in Brazilian Amazonia: history, rates, and consequences. *Conserv. Biol.* 19, 680–688. doi: 10.1111/j.1523-1739.2005.00697.x

Fonseca, M. G., Anderson, L. O., Arai, E., Shimabukuro, Y. E., Xaud, H. A. M., Xaud, M. R., et al. (2017). Climatic and anthropogenic drivers of northern Amazon fires during the 2015-2016 El Niño event. *Ecol. Appl.* 27, 2514–2527. doi: 10.1002/eap.1628

Funk, C., Peterson, P., Landsfeld, M., Pedreros, D., Verdin, J., Shukla, S., et al. (2015). The climate hazards infrared precipitation with stations—a new environmental record for monitoring extremes. *Sci. Data* 2:150066. doi: 10.1038/sdata.2015.66

Garcia, B., Libonati, R., and Nunes, A. (2018). Extreme drought events over the amazon basin: the perspective from the reconstruction of South American hydroclimate. *Water* 10:1594. doi: 10.3390/w10111594

Giglio, L., Descloitres, J., Justice, C. O., and Kaufman, Y. J. (2003). An enhanced contextual fire detection algorithm for MODIS. *Remote Sens. Environ.* 87, 273–282. doi: 10.1016/S0034-4257(03)00184-6

Giglio, L., Randerson, J. T., van der Werf, G. R., van der Werf, G. R., and van der Werf, G. R. (2013). Analysis of daily, monthly, and annual burned area using the fourth-generation global fire emissions database (GFED4). *J. Geophys. Res. Biogeosci.* 118, 317–328. doi: 10.1002/jgrg.20042

Giglio, L., Schroeder, W., and Justice, C. O. (2016). The collection 6 MODIS active fire detection algorithm and fire products. *Remote Sens. Environ.* 178, 31–41. doi: 10.1016/j.rse.2016.02.054

Hilker, T., Lyapustin, A. I., Tucker, C. J., Hall, F. G., Myneni, R. B., Wang, Y., et al. (2014). Vegetation dynamics and rainfall sensitivity of the Amazon. *Proc. Natl. Acad. Sci. U.S.A.* 111, 16041–16046. doi: 10.1073/pnas.1404870111

Instituto Brasileiro de Geografia e Estatística [IBGE] (2004). *Mapa de Biomas e de Vegetação*. Available at: http://www.ibge.gov.br/home/presidencia/noticias/21052004biomashtml.shtm (accessed March 22, 2015).

Instituto Nacional de Pesquisas Espaciais [INPE] (2018). *PRODES - Monitoramento da Floresta Amazônica Brasileira Por Satélite*. Available at: http://www.obt.inpe.br/prodes/ (accessed January 1, 2018).

Jimenez, J. C., Libonati, R., and Peres, L. F. (2018). Droughts over amazonia in 2005, 2010, and 2015: a cloud cover perspective. *Front. Earth Sci.* 6, 1–7. doi: 10.3389/feart.2018.00227

Jiménez-Muñoz, J. C., Mattar, C., Barichivich, J., Santamaría-Artigas, A., Takahashi, K., Malhi, Y., et al. (2016). Record-breaking warming and extreme drought in the Amazon rainforest during the course of El Niño 2015–2016. *Sci. Rep.* 6:33130. doi: 10.1038/srep33130

Kalamandeen, M., Gloor, E., Mitchard, E., Quincey, D., Ziv, G., Spracklen, D., et al. (2018). Pervasive rise of small-scale deforestation in Amazonia. *Sci. Rep.* 8:1600. doi: 10.1038/s41598-018-19358-2

Katsanos, D., Retalis, A., and Michaelides, S. (2016). Validation of a high-resolution precipitation database (CHIRPS) over Cyprus for a 30-year period. *Atmos. Res.* 169, 459–464. doi: 10.1016/j.atmosres.2015.05.015

Köppen, W. (1936). "Das geographische system der klimate," in *Handbuch der klimatologie*, eds W. Köppen and R. Geiger (Berlin: Gebruder Borntraeger), 1–44.

Kottek, M., Grieser, J., Beck, C., Rudolf, B., and Rubel, F. (2006). World Map of the Köppen-Geiger climate classification updated. *Meteorol. Zeitschrift* 15, 259–263. doi: 10.1127/0941-2948/2006/0130

Lewis, S. L., Brando, P. M., Phillips, O. L., van der Heijden, G. M. F., and Nepstad, D. (2011). The 2010 amazon drought. *Science* 331, 554–554. doi: 10.1126/science.1200807

Li, W., Fu, R., and Dickinson, R. E. (2006). Rainfall and its seasonality over the Amazon in the 21st century as assessed by the coupled models for the IPCC AR4. *J. Geophys. Res.* 111:D02111. doi: 10.1029/2005JD006355

Lima, A., Silva, T. S. F., Aragão, L. E., De Feitas, R. M., Adami, M., Formaggio, A. R., et al. (2012). Land use and land cover changes determine the spatial relationship between fire and deforestation in the Brazilian Amazon. *Appl. Geogr.* 34, 239–246. doi: 10.1016/j.apgeog.2011.10.013

Lima, C. H. R., AghaKouchak, A., and Randerson, J. T. (2018). Unraveling the role of temperature and rainfall on active fires in the Brazilian Amazon using a nonlinear poisson model. *J. Geophys. Res. Biogeosci.* 123, 117–128. doi: 10.1002/2017JG003836

Lopez-Carr, D., Mwenda, K. M., Pricope, N. G., Kyriakidis, P. C., Jankowska, M. M., Weeks, J., et al. (2015). "A spatial analysis of climate-related child malnutrition in the Lake Victoria Basin," in *Proceedings of the 2015 IEEE International Geoscience and Remote Sensing Symposium (IGARSS)*, (Milan: IEEE), 2564–2567.

Malhi, Y., Roberts, J. T., Betts, R. A., Killeen, T. J., Li, W., and Nobre, C. A. (2008). Climate change, deforestation, and the fate of the amazon. *Science* 319, 169–172. doi: 10.1126/science.1146961

Mantua, N. J., Hare, S. R., Zhang, Y., Wallace, J. M., and Francis, R. C. (1997). A pacific interdecadal climate oscillation with impacts on salmon production. *Bull. Am. Meteorol. Soc.* 78, 1069-1079

MapBiomas (2018). *Project MapBiomas - Collection 3 of Brazilian Land Cover & Use Map Series*. Available at: http://mapbiomas.org/ (accessed September 20, 2018).

Marengo, J. A., and Betts, R. (eds) (2011). *Riscos das Mudanças Climáticas no Brasil: análise conjunta Brasil-Reino Unido sobre os impactos das mudanças climáticas e do desmatamento na Amazônia*. São José dos Campos: CCST/INPE.

Marengo, J. A., and Espinoza, J. C. (2016). Extreme seasonal droughts and floods in Amazonia: causes, trends and impacts. *Int. J. Climatol.* 36, 1033–1050. doi: 10.1002/joc.4420

Marengo, J. A., Souza, C. A., Thonicke, K., Burton, C., Halladay, K., Betts, R. A., et al. (2018). Changes in climate and land use over the amazon region: current and future variability and trends. *Front. Earth Sci.* 6:228. doi: 10.3389/feart.2018.00228

Marengo, J. A., Tomasella, J., Alves, L. M., Soares, W. R., and Rodriguez, D. A. (2011). The drought of 2010 in the context of historical droughts in the Amazon region. *Geophys. Res. Lett.* 38, 1–5. doi: 10.1029/2011GL047436

Marengo, J. A., Williams, E. R., Alves, L. M., Soares, W. R., and Rodriguez, D. A. (2016). "Extreme seasonal climate variations in the amazon basin: droughts and floods," in *Interactions Between Biosphere, Atmosphere and Human Land Use in the Amazon Basin*, eds L. Nagy, B. R. Forsberg, and P. Artaxo (Berlin: Springer), 55–76. doi: 10.1007/978-3-662-49902-3_4

Martins, V. S., Novo, E. M. L. M., Lyapustin, A., Aragão, L. E. O. C., Freitas, S. R., and Barbosa, C. C. F. (2018). Seasonal and interannual assessment of cloud cover and atmospheric constituents across the Amazon (2000–2015): insights for remote sensing and climate analysis. *ISPRS J. Photogramm. Remote Sens.* 145, 309–327. doi: 10.1016/j.isprsjprs.2018.05.013

Maués, M. M., and Oliveira, P. E. A. M. (2010). Consequências da fragmentação do habitat na ecologia reprodutiva de espécies arbóreas em florestas tropicais, com ênfase na Amazônia. *Oecologia Aust.* 14, 238–250. doi: 10.4257/oeco.2010.1401.14

McGregor, S., Timmermann, A., Stuecker, M. F., England, M. H., Merrifield, M., Jin, F.-F., et al. (2014). Recent Walker circulation strengthening and Pacific cooling amplified by Atlantic warming. *Nat. Clim. Chang.* 4, 888–892. doi: 10.1038/nclimate2330

Ministério do Meio Ambiente [MMA] (2018). *Amazônia*. Available at: http://www.mma.gov.br/biomas/amazônia (accessed January 1, 2018).

Morton, D. C., Defries, R. S., Shimabukuro, Y. E., Anderson, L. O., Arai, E., Espirito-santo, B., et al. (2006). Cropland expansion changes deforestation dynamics in the southern Brazilian Amazon. *Proc Natl Acad Sci U S A.* 103, 14637–14641. doi: 10.1073/pnas.0606377103

Moura, Y. M., de Hilker, T., Lyapustin, A. I., Galvão, L. S., dos Santos, J. R., Anderson, L. O., et al. (2015). Seasonality and drought effects of Amazonian forests observed from multi-angle satellite data. *Remote Sens. Environ.* 171, 278–290. doi: 10.1016/j.rse.2015.10.015

Nepstad, D., Lefebvre, P., Lopes da Silva, U., Tomasella, J., Schlesinger, P., Solorzano, L., et al. (2004). Amazon drought and its implications for forest flammability and tree growth: a basin-wide analysis. *Glob. Chang. Biol.* 10, 704–717. doi: 10.1111/j.1529-8817.2003.00772.x

Nepstad, D., Soares-Filho, B. S., Merry, F., Lima, A., Moutinho, P., Carter, J., et al. (2009). The end of deforestation in the Brazilian Amazon. *Science* 326, 1350–1351. doi: 10.1126/science.1182108

Nepstad, D. C., Tohver, I. M., Ray, D., Moutinho, P., and Cardinot, G. (2007). Mortality of large trees and lianas following experimental drought in an Amazon forest. *Ecology* 88, 2259–2269. doi: 10.1890/06-1046.1

NPCC-Interministerial Committee on Climate Change (2008). *Interministerial Committee on Climate Change and National Plan on Climate Change-Decree No. 6263*. Brazil: National Policy on Climate Change.

Panisset, J. S., Libonati, R., Gouveia, C. M. P., Machado-Silva, F., França, D. A., França, J. R. A., et al. (2018). Contrasting patterns of the extreme drought episodes of 2005, 2010 and 2015 in the amazon basin. *Int. J. Climatol.* 38, 1096–1104. doi: 10.1002/joc.5224

Perdigón-Morales, J., Romero-Centeno, R., Pérez, P. O., and Barrett, B. S. (2018). The midsummer drought in Mexico: perspectives on duration and intensity from the CHIRPS precipitation database. *Int. J. Climatol.* 38, 2174–2186. doi: 10.1002/joc.5322

Phillips, O. L., Aragao, L. E., Lewis, S. L., Fisher, J. B., Lloyd, J., Lopez-Gonzalez, G., et al. (2009). Drought sensitivity of the amazon rainforest. *Science* 323, 1344–1347. doi: 10.1126/science.1164033

Randerson, J. T., Chen, Y., van der Werf, G. R., Rogers, B. M., and Morton, D. C. (2012). Global burned area and biomass burning emissions from small fires. *J. Geophys. Res. Biogeosci.* 117:G04012. doi: 10.1029/2012JG002128

Saatchi, S., Asefi-Najafabady, S., Malhi, Y., Aragao, L. E., Anderson, L. O., Myneni, R. B., et al. (2013). Persistent effects of a severe drought on Amazonian forest canopy. *Proc. Natl. Acad. Sci. U.S.A.* 110, 565–570. doi: 10.1073/pnas.1204651110

Schlesinger, M. E., and Ramankutty, N. (1994). An oscillation in the global climate system of period 65–70 years. *Nature* 367, 723–726. doi: 10.1038/367723a0

Silva Junior, C., Almeida, C., Santos, J., Anderson, L., Aragão, L., and Silva, F. (2018a). Spatiotemporal rainfall trends in the Brazilian legal amazon between the years 1998 and 2015. *Water* 10:1220. doi: 10.3390/w10091220

Silva Junior, C., Aragão, L., Fonseca, M., Almeida, C., Vedovato, L., and Anderson, L. (2018b). Deforestation-induced fragmentation increases forest fire occurrence in Central Brazilian Amazonia. *Forests* 9:305. doi: 10.3390/f9060305

Smith, L. T., Aragão, L. E., Sabel, C. E., and Nakaya, T. (2014). Drought impacts on children's respiratory health in the Brazilian Amazon. *Sci. Rep.* 4:3726. doi: 10.1038/srep03726

Van Der Werf, G. R., Randerson, J. T., Giglio, L., Collatz, G. J., Mu, M., Kasibhatla, P. S., et al. (2010). Global fire emissions and the contribution of deforestation, savanna, forest, agricultural, and peat fires (1997-2009). *Atmos. Chem. Phys.* 10, 11707–11735. doi: 10.5194/acp-10-11707-2010

Van Der Werf, G. R., Randerson, J. T., Giglio, L., van Leeuwen, T. T., Chen, Y., Rogers, B. M., et al. (2017). Global fire emissions estimates during 1997–2016. *Earth Syst. Sci. Data* 9, 697–720. doi: 10.5194/essd-9-697-2017

Verdin, A., Funk, C., Rajagopalan, B., and Kleiber, W. (2016). Kriging and local polynomial methods for blending satellite-derived and gauge precipitation estimates to support hydrologic early warning systems. *IEEE Trans. Geosci. Remote Sens.* 54, 2552–2562. doi: 10.1109/TGRS.2015.2502956

Wan, Z., Hook, S., and Hulley, G. (2015). *MOD11C3 MODIS/Terra Land Surface Temperature/Emissivity Monthly L3 Global 0.05Deg CMG V006. NASA EOSDIS L. Process. DAAC*. Washington, DC: National Aeronautics and Space Administration.

Withey, K., Berenguer, E., Palmeira, A. F., Espírito-Santo, F. D. B., Lennox, G. D., Silva, C. V. J., et al. (2018). Quantifying immediate carbon emissions from El Niño-mediated wildfires in humid tropical forests. *Philos. Trans. R. Soc. B Biol. Sci.* 373:20170312. doi: 10.1098/rstb.2017.0312

Wolter, K. (1987). The southern oscillation in surface circulation and climate over the tropical atlantic, eastern pacific, and indian oceans as captured by cluster analysis. *J. Clim. Appl. Meteorol.* 26, 540–558. doi: 10.1175/1520-04501987026<0540:TSOISC<2.0.CO;2

Wolter, K., and Timlin, M. S. (2011). El Niño/southern oscillation behaviour since 1871 as diagnosed in an extended multivariate ENSO index (MEI.ext). *Int. J. Climatol.* 31, 1074–1087. doi: 10.1002/joc.2336

Zhang, Y., Wallace, J. M., and Battisti, D. S. (1997). ENSO-like interdecadal variability: 1900-93. *J. Clim.* 10, 1004–1020. doi: 10.1175/1520-04421997010<1004:ELIV<2.0.CO;2

Conflict of Interest Statement: The authors declare that the research was conducted in the absence of any commercial or financial relationships that could be construed as a potential conflict of interest.